A Targeted Library of Small-Molecule, Tyrosine, and Dual-Specificity Phosphatase Inhibitors Derived from a Rational Core Design and Random Side Chain Variation†

Robert L. Rice,‡ James M. Rusnak,‡ Fumiaki Yokokawa,§ Shiho Yokokawa,§ Donald J. Messner,|| Alton L. Boynton,|| Peter Wipf,§ and John S. Lazo*,‡

Departments of Pharmacology and Chemistry, University of Pittsburgh, Pittsburgh, Pennsylvania 15261, and Department of Molecular Medicine, Northwest Hospital, Seattle, Washington 98125

Received June 5, 1997; Revised Manuscript Received August 25, 1997⊗

ABSTRACT: Tyrosine phosphatases (PTPases) dephosphorylate phosphotyrosines while dual-specificity phosphatases (DSPases) dephosphorylate contiguous and semicontiguous phosphothreonine and phosphotyrosine on cyclin dependent kinases and mitogen-activated protein kinases. Consequently, PTPases and DSPases have a central role controlling signal transduction and cell cycle progression. Currently, there are few readily available potent inhibitors of PTPases or DSPases other than vanadate. Using a pharmacophore modeled on natural product inhibitors of phosphothreonine phosphatases, we generated a refined library of novel, phosphate-free, small-molecule compounds synthesized by a parallel, solid-phase combinatorial-based approach. Among the initial 18 members of this targeted diversity library, we identified several inhibitors of DSPases: Cdc25A, -B, and -C and the PTPase PTP1B. These compounds at 100 μM did not significantly inhibit the protein serine/threonine phosphatases PP1 and PP2A. Kinetic studies with two members of this library indicated competitive inhibition for Cdc25 DSPases and noncompetitive inhibition for PTP1B. Compound AC-αα69 had a K_i of approximately 10 μM for recombinant human Cdc25A, -B, and -C, and a K_i of 0.85 μM for the PTP1B. The marked differences in Cdc25 inhibition as compared to PTP1B inhibition seen with relatively modest chemical modifications in the modular side chains demonstrate the structurally demanding nature of the DSPase catalytic site distinct from the PTPase catalytic site. These results represent the first fundamental advance toward a readily modifiable pharmacophore for synthetic PTPase and DSPase inhibitors and illustrate the significant potential of a combinatorial-based strategy that supplements the rational design of a core structure by a randomized variation of peripheral substituents.

Reversible covalent modification of proteins by the addition and removal of phosphate residues dominates as the method used by mammalian cells in intracellular signaling. A complex cascade of interrelated protein kinases and protein phosphatases dynamically regulate intracellular protein phosphorylation. Two broad families of eukaryotic protein phosphatases have been defined: protein serine/threonine phosphatases (PSTPase)[1] and protein tyrosine phosphatases (PTPase). More recently a subfamily of PTPases, the dual-specificity phosphatases (DSPase), has been identified, which dephosphorylate tyrosine and threonine residues on the same substrate (*1*). Two major members of the DSPase family are the Cdc25 phosphatases, which dephosphorylate a contiguous TY motif, and the mitogen-activated protein kinase (MAPK) phosphatases, which dephosphorylate a semicontiguous TXY, where X is G, P, or E.

Investigation of the biological role of PSTPases has been greatly facilitated by the discovery of natural low-molecular weight enzyme inhibitors. Okadaic acid, a polyether fatty acid produced by a marine dinoflagellate, was the first broadly characterized PSTPase inhibitor, and more recently other natural products, such as microcystins and calyculin A, also have been found to be excellent active site inhibitors (*2*−*5*). These potent PSTPase inhibitors are widely used to decipher intracellular signal transduction pathways, but all have limitations such as poor cell permeability, chemical instability, and finite supply. Moreover, the known PSTPase inhibitors also have restricted PSTPase isotype specificity and have little, if any, activity toward PTPases. Studies of the intracellular function of PTPases and particularly DSPases have been severely hampered by the lack of potent inhibitors. Vanadate, which has been widely used as an inhibitor of both PTPases and DSPases, is one of the few

† This work was supported in part by Army Breast Cancer Predoctoral Research Fellowship DAMD17-94-J4193, the Fiske Drug Discovery Fund, and USPHS NIH Grants CA 61299, CA 39745, CA 53861, and AI 34914.

* Address correspondence to this author at Department of Pharmacology, Biomedical Science Tower E-1340, University of Pittsburgh, Pittsburgh, PA 15261. Telephone: (412) 648-9319. Fax: (412) 648-2229. E-mail: lazo@pop.pitt.edu.

‡ Department of Pharmacology, University of Pittsburgh.

§ Department of Chemistry, University of Pittsburgh.

|| Northwest Hospital.

⊗ Abstract published in *Advance ACS Abstracts,* December 1, 1997.

[1] Abbreviations: AEBSF, 4-(2-aminoethyl)benzenesulfonyl fluoride; BopCl, bis(2-oxo-3-oxazolidinyl)phosphinic chloride; DPPA, diphenylphosphoryl azide; DSPases, dual-specificity phosphatases; DTT, DL-dithiothreitol; FDP, 3,6-fluorescein diphosphate; GST, glutathione-S-transferase; IC_{50}, half-maximal inhibitory concentration; IPTG, isopropyl β-D-thiogalactopyranoside; MAPK, mitogen-activated protein kinase; MAPKP, mitogen-activated protein kinase phosphatase; pNPP, *para*-nitrophenyl phosphate; SC, solution chemistry; PSTPases, protein serine/threonine phosphatases; PTPases, protein tyrosine phosphatases.

S0006-2960(97)01338-X CCC: $14.00

inhibitors readily available (*6*−*9*). For several DSPases, namely Cdc25A and -B, the endogenous substrates are not known. The natural products dnacin, dysidiolide, and a RK-682 analogue appear to inhibit Cdc25 DSPases (*9*−*11*), but there is little information on the nature of their inhibition, their selectivity, or their cell permeability, and, as they are natural products, limited supplies restrict their widespread use. The best reported inhibitor of PTPase is a competitive cyclic peptide inhibitor with a K_i of 0.73 μM that has the disadvantages associated with a peptide inhibitor (*12*). Thus, good artificial inhibitors would facilitate analyses of the biological role of PTPases and DSPases.

Although some investigators have reported structural similarities between the PSTPases and DSPases (*13*), recent thoughtful analyses of the active site structures of protein phosphatases (*1, 14, 15*) suggest that sufficient differences exist among the protein phosphatase classes to permit the identification of selective inhibitors. Thus, we have begun to devise strategies to generate selective, small-molecule, active site inhibitors of protein phosphatases. We purposefully focused on small molecules and excluded phosphates in our design to enhance the likelihood that the resulting compounds would enter cells. In our initial attempt to generate PSTPase isotype selective inhibitors, a core moiety for phosphatase inhibition was chosen based on the readily available structure−activity relationship profile for natural product PSTPase inhibitors (*16*, *17*). To complement this design, we adapted a combinatorial synthetic approach for the random variation of substituents to ensure chemical diversity and maximum flexibility. We synthesized an initial library on solid support to establish the overall synthetic approach and documented that at least one member of the library retained some ability to inhibit the PSTPase PP2A (*17*). In the current study we have markedly extended our analysis to include the entire library and a significant number of protein phosphatases, namely, the PSTPases PP1 and PP2A, the DSPases Cdc25A, Cdc25B, Cdc25C, and CL100, and the PTPase PTP1B. Surprisingly, among the initial 18 members of the targeted diversity library, we identified several competitive inhibitors of Cdc25 phosphatase and noncompetitive inhibitors of PTP1B that have little activity against the PSTPase PP1 and PP2A. These results represent the first fundamental advance toward identifying a readily modifiable pharmacophore for the design of nonelectrophilic, small-molecule PTPase and DSPase inhibitors. Moreover, the marked differences in Cdc25 inhibition as compared to PTP1B inhibition seen with relatively modest chemical modifications in modular side chains demonstrate the structurally demanding nature of the DSPase active site that was distinct from the PTP1B catalytic site.

MATERIALS AND METHODS

Chemical Compounds. The generation of the compounds in the combinatorial library has been previously described (*17*), although we have now adopted a new, more descriptive nomenclature for ease of discussion. The new nomenclature and the compound structures are listed in Figure 1 and Table 1. The basic combinatorial pharmacophore is now termed AC (Figure 1); addition of a phenyl moiety is termed α, a phenethyl is β, benzyl is δ, a styryl is γ, and alkyl chains are designated on the basis of the carbon length. Compounds were synthesized using solid bead combinatorial methods, and their predicted structural identity and purity (>60%) were

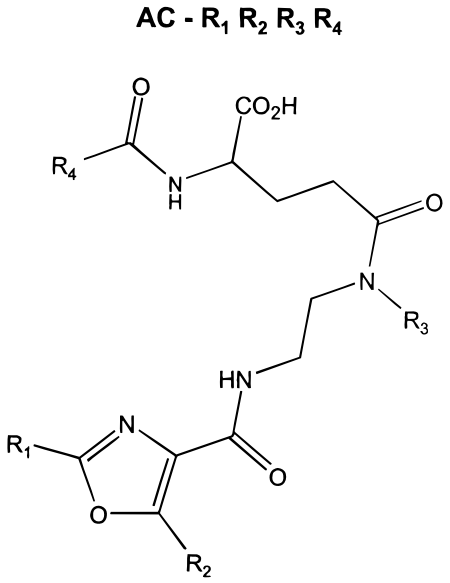

FIGURE 1: General chemical structure of pharmacophore.

Table 1

Compound	R_1	R_2	R_3	R_4
AC-α119	⬡	CH_3	CH_3	n-C_9H_{19}
AC-α169	⬡	CH_3	n-C_6H_{13}	n-C_9H_{19}
AC-α1δ9	⬡	CH_3	⬡	n-C_9H_{19}
AC-αα19	⬡	⬡	CH_3	n-C_9H_{19}
AC-αα69	⬡	⬡	n-C_6H_{13}	n-C_9H_{19}
AC-ααδ9	⬡	⬡	⬡	n-C_9H_{19}
AC-α11β	⬡	CH_3	CH_3	⬡
AC-α16β	⬡	CH_3	n-C_6H_{13}	⬡
AC-α1δβ	⬡	CH_3	⬡	⬡
AC-αα1β	⬡	⬡	CH_3	⬡
AC-αα6β	⬡	⬡	n-C_6H_{13}	⬡
AC-ααδβ	⬡	⬡	⬡	⬡
AC-α11γ	⬡	CH_3	CH_3	⬡
AC-α16γ	⬡	CH_3	n-C_6H_{13}	⬡
AC-α1δγ	⬡	CH_3	⬡	⬡
AC-αα1γ	⬡	⬡	CH_3	⬡
AC-αα6γ	⬡	⬡	n-C_6H_{13}	⬡
AC-ααδγ	⬡	⬡	⬡	⬡

confirmed by ^{1}H NMR and mass spectroscopy (*17*). Several discrete compounds, namely, AC-ααδ9 and AC-αα69, were synthesized using solution chemistry (SC) according to (*17*) and are referred to as SC compounds throughout this manuscript to differentiate them from compounds synthesized by solid bead-based combinatorial methods. For the resynthesis of these compounds, 2,2,2-trichlorethoxycarbonyl and allyloxycarbonyl protective groups were used, and amide coupling was effected with BopCl (*18*) and DPPA (*19*) coupling agents. We also synthesized for the first time SC-α109 and SC-αα09 for structural hypothesis testing and used the same procedure as mentioned above for SC-ααδ9 and SC-αα69. The SC compounds were >90% pure on the basis

of previously described ^{1}H NMR and mass spectroscopy methods (*17*). All compounds were resuspended for biological testing in DMSO as a stock solution of 10 mM and stored in the dark at −70 °C in aliquots for use in individual experiments. In contrast to the solid-phase library, which was enriched in the L-stereoisomers, the SC compounds were racemic.

Plasmids and Reagents. Plasmid pGEX2T for glutathione-*S*-transferase (GST) fusion of full-length human Cdc25A was a gift from Dr. Robert T. Abraham (Mayo Clinic, Rochester, MN), and the plasmids pGEX2T-KG and pGEX2T containing the GST fusion of full-length human Cdc25B and -C, respectively, were a gift from Dr. David Beach (Cold Spring Harbor Laboratory, Cold Spring Harbor, NY). The plasmid pET15b containing the histidine-tagged CL100 was a gift from Dr. Stephen M. Keyse (University of Dundee, Dundee, U.K.). The substrate 3,6-fluorescein diphosphate (FDP) was purchased from Molecular Probes Inc. (Eugene, OR), *para*-nitrophenyl phosphate (pNPP) was obtained from Sigma (St. Louis, MO), and Ni-NTA was purchased from Qiagen Inc (Chatsworth, CA). The inhibitory activity of SC-ααδ9 and SC-αα69 against PP1 and PP2A was measured with the phosphatase assay kit from Gibco-BRL (Grand Island, NY) using PP1 and PP2A catalytic units purified from rabbit skeletal muscle obtained from Upstate Biotechnology (Lake Placid, NY). Phosphorylase *b* was radiolabeled with Redivue [^{32}P]γATP, which was from Amersham (Arlington Heights, IL). Alkaline phosphatase from calf intestine was purchased from Promega (Madison, WI). Recombinant PTP1B was obtained from Upstate Biotechnology (Lake Placid, NY).

Bacterial Growth and Fusion Protein Production. Escherichia coli strain BL21 (DE3) was used for transfection with plasmids containing the fusion constructs encoding GST and Cdc25A, -B, or -C under the transcriptional control of isopropyl β-D-thiogalactopyranoside (IPTG). *E. coli* were first grown overnight at 37 °C in the presence of LB media with 100 μg/mL ampicillin. A 4 mL aliquot of this preculture was used to inoculate 1 L of LB containing 100 μg/mL of ampicillin. The cultures were incubated at 37 °C for 4−5 h. IPTG (1 mM final concentration) was then added, and the cultures were incubated at 37 °C for an additional 3 h. Cells were harvested by centrifugation at 3500*g* for 10 min at 4 °C. The resultant bacterial pellets were kept frozen at −80 °C until extraction. His_6-tagged CL100 was produced similarly except the *E. coli* strain DH5a was used in place of BL21 (DE3).

Purification of GST Fusion Proteins. The bacterial pellet was disrupted by sonication at 4 °C in lysis buffer containing 10 μg/mL of aprotinin, 10 μg/mL of leupeptin, 100 μg/mL of AEBSF, and 10 mM DTT. The homogenate was then centrifuged for 10 min at 4 °C at 10000*g*. The resulting supernatant fraction was immediately mixed and rotated with glutathione beads (equilibrated with lysis buffer) for 1 h at 4 °C (5 vol of supernatant/1 vol of 50% bead slurry). The glutathione beads were washed two times with 10 vol of lysis buffer and then twice with 10 vol of 2× reaction buffer (60 mM Tris, pH 8.5, 150 mM NaCl, 1.34 mM EDTA, 0.066% BSA) containing 10 μg/mL of aprotinin, 10 μg/mL of leupeptin, 100 μg/mL of AEBSF, and 10 mM DTT. The fusion protein was eluted with three successive washes using 10 mM glutathione in 2× reaction buffer. The efficiency of the elution was monitored by the phosphatase assay described below. Active fractions were pooled and supplemented with 20% glycerol prior to storage at −80 °C. His_6-tagged CL100 was purified using the same procedure except 20 mM β-mercaptoethanol was used in place of DTT for all steps of the purification and 100 mM imidazole was used instead of 10 mM glutathione for the elution.

Serine/Threonine Phosphatase Assay. The catalytic subunits of PP1 and PP2A were purified from oysters and phosphatase activity was determined with a radiolabeled phosphohistone substrate (histone HI) was determine by the liberation of ^{32}P using previously described procedures (*20, 21*). Briefly, assays were conducted in a final volume of 80 μL containing 50 mM Tris buffer (pH 7.4), 0.5 mM DTT, 1 mM EDTA (assay buffer), phosphohistone (1−2 μM PO_4), and the catalytic subunits of either PP1 or PP2A. Okadaic acid (1 nM) was included in some PP1 preparations to suppress endogenous PP2A activity and had no apparent affect on the inhibitory activity of the compounds tested. Dephosphorylation of ^{32}P-labeled histone was determined after a 10−20 min incubation with or without 100 μM combinatorial compounds by extraction as a phosphomolybdate complex as described previously (*20, 21*). The reaction was directly dependent on enzyme concentration and time under these conditions. The inhibitory activity of SC-ααδ9 and SC-αα69 against PP1 and PP2A was also measured with rabbit skeletal muscle PP1 and PP2A and ^{32}P-labeled phosphorylase A as a substrate by the commercially available method of Gibco-BRL.

PTPase and Dual-Specificity Phosphatase Assay. The activity of the GST fusion or His_6-tagged DSPase and PTPase was measured with FDP (Molecular Probes, Inc., Eugene, OR), which is readily metabolized to the fluorescent fluorescein monophosphate (*7*), as a substrate in a 96-well microtiter plates. The final incubation mixture (150 μL) comprised 30 mM Tris (pH 8.5), 75 mM NaCl, 0.67 mM EDTA, 0.033% bovine serum albumin, 1 mM DTT, and 20 μM FDP for Cdc25 phosphatases. The same final incubation mixture was used for CL100 and PTP1B, with the appropriate pH optimum, namely, pH 7.0 and 7.5, respectively. Inhibitors were resuspended in DMSO, and all reactions including controls were performed at a final concentration of 7% DMSO. Reactions were initiated by adding ∼0.25 μg of fusion protein and incubated at ambient temperature for 1 h for Cdc25 and CL100 phosphatase and 30 min for PTP1B. Fluorescence emission from the product was measured with a multiwell plate reader (Perseptive Biosystems Cytofluor II, Framingham, MA; excitation filter, 485/20; emission filter, 530/30). For all enzymes the reaction was linear over 2 h of incubation, well within the time used in the experiments, and was directly proportional to both the enzyme and substrate concentration.

Alkaline Phosphatase Assay. The activity of alkaline phosphatase was measured in a 96-well microtiter plate with FDP (Molecular Probes, Inc., Eugene, OR) as a substrate, which was readily metabolized to the fluorescent fluorescein monophosphate (*7*). The final incubation mixture (150 μL) contained 30 mM Tris (pH 7.3), 75 mM NaCl, 0.67 mM EDTA, 0.033% bovine serum albumin, 1 mM DTT, and 1 μM FDP ($\sim K_m$). Inhibitors were resuspended in DMSO, and all reactions including controls were performed at a final concentration of 7% DMSO. Reactions were initiated by adding ∼0.1 unit of alkaline phosphatase and incubated at ambient temperature for 5 min. Fluorescence emission from the product was measured with a multiwell plate reader (Perseptive Biosystems Cytofluor II, Framingham, MA;

excitation filter, 485/20; emission filter, 530/30). For all enzymes the reaction was linear over the time of incubation and directly proportional to both the enzyme and substrate concentration.

Thin-Layer Chromatography. To ensure that only a single product was produced with the FDP substrate, we incubated FDP and phosphatases under our standard reaction conditions for 0.5 to 1 h and spotted 2.5 μL of the reaction from each microtiter plate well on a Whatman reversed phase TLC LKC_{18} plate. The resolving conditions were room temperature and a methanol/water (3:2 vol) solvent. Compounds and products were viewed under long UV wavelength (366 nm) to illuminate the potential fluorescein monophosphate and fluorescein product. FDP has no fluorescent intensity at this wavelength. The R_f values for fluorescein monophosphate and fluorescein were 0.9 and 0.8, respectively. We found that only the fluorescein monophosphate was produced under our reaction conditions with the PTPase and DSPases used. Thus, despite the ability of Cdc25 to dephosphorylate fluorescein monophosphate (*22*), under the reaction conditions used the diphosphate fluorescein was the preferred substrate as previously suggested (*13*).

Steady-State Kinetics. Reactions with GST-Cdc25A, -B, and -C were conducted in 30 mM Tris (pH 8.5), 75 mM NaCl, 0.67 mM EDTA, 0.033% bovine serum albumin, and 1 mM DTT. Reactions with CL100 were conducted in 30 mM Tris (pH 7.0), 75 mM NaCl, 0.67 mM EDTA, 0.033% BSA, 1 mM DTT, and 20 mM imidazole. Reactions with GST-PTP1B were conducted in 30 mM Tris (pH 7.5), 75 mM NaCl, 0.67 mM EDTA, 0.033% bovine serum albumin, and 1 mM DTT. DMSO was kept at 7% in reaction mixtures to ensure compound solubility. All reactions were carried out at room temperature, and product formation was determined in an multiwell plate reader (Perseptive Biosystems Cytofluor II, Framingham, MA; excitation filter, 485/20; emission filter, 530/30). Data were collected at 10 min intervals for 1 h for Cdc25 and CL100 phosphatases and 30 min for PTP1B. The V_0 was determined for each substrate concentration and then fit to the Michaelis−Menten equation (eq 1):

$$V_o = V_{max}[S]/(K_m + [S]) \quad (1)$$

using Prism 2.01 (GraphPad Software Inc.). The correlation coefficient for each experiment and substrate concentration was always >0.9. The substrate concentrations used to determine the steady-state kinetics for Cdc25A, -B, and -C were 10, 20, 30, 40, 50, 75, 100, and 200 mM FDP; for CL100 the concentrations were 75, 100, 200, 300, 400, 500, and 750 μM FDP; and for PTP1B the concentrations were 1, 5, 10, 25, 50, 75, 100, 150 μM FDP.

Determination of Inhibition Constant. The inhibition constants for SC-ααδ9 and SC-αα69 were determined for the Cdc25A, -B, and -C, CL100, and PTP1B hydrolysis of FDP. At various fixed concentrations of inhibitor, the initial rates with different concentrations of FDP were measured. The data were then fit to eq 2 to obtain the inhibition constant (K_i) for the competitive model or eq 3 for the noncompetitive model.

$$V_o = V_{max}[S]/(K_m(1 + [I]/K_i) + [S]) \quad (2)$$

$$V_o = V_{max}[S]/((K_m + [S])(1 + [I]/K_i)) \quad (3)$$

Table 2: Percent Inhibition of PSTPase Activity with 100 μM Combinatorial Compound[a]

	PP1		PP2A	
compound	mean	SEM	mean	SEM
AC-α119	0	0	0	0
AC-α169	4	10	14	15
AC-α1δ9	11	3	33	13
AC-αα19	0	0	0	0
AC-αα69	0	0	0	0
AC-ααδ9	9	7	5	11
AC-α11β	12	6	15	11
AC-α16β	11	5	31	10
AC-α1$\delta\beta$	13	1	48	8
AC-αα1β	22	2	20	4
AC-αα6β	1	19	32	21
AC-αα$\delta\beta$	32	5	47	6
AC-α11γ	11	4	13	4
AC-α16γ	27	9	23	2
AC-α1$\delta\gamma$	25	3	35	4
AC-αα1γ	27	5	8	11
AC-αα6γ	17	9	40	9
AC-αα$\delta\gamma$	24	9	46	8

[a] Each value is the percent inhibition from untreated control and the mean from three independent determinations.

At least four concentrations of SC-ααδ9 and SC-αα69 ranging from 0 to 30 μM were used with Cdc25A or -B. The K_i of Cdc25C was calculated using at least 4 concentrations of drugs that ranged from 0 to 100 μM of SC-αα69 and SC-ααδ9. At least four concentrations of SC-ααδ9 and SC-αα69 ranging from 0 to 3 μM were used with PTP1B. The K_i of CL100 was determined using three different concentrations of SC-ααδ9: 30, 100, and 300 μM.

RESULTS AND DISCUSSION

Phosphatase Inhibition by Solid Phase-Derived Compounds. All members of the current library contained a phenyl substituent on the oxazole C_2 (i.e., R_1) (Table 1). Because the fundamental pharmacophore was based on the PSTPase inhibitors calyculin A, microcystins, and okadaic acid, we initially examined the library for its ability to disrupt two established PSTPases. One-third of the library members completely failed to inhibit PP1 at 100 μM (Table 2) while more than two-thirds of the library members inhibited PTP1B with >50% inhibition at 100 μM (Table 4). Several compounds demonstrated >40% inhibition of PTP1B at 3 μM. Only modest inhibition of PP1 was observed with most library compounds and the maximum reduction in PP1 activity of 32% was seen with AC-αα$\delta\beta$, which interestingly was the one compound that failed to inhibit PTP1B at 100 μM (Table 4). We found at 100 μM approximately one-third of the library members caused >30% inhibition of PP2A with AC-α1$\delta\beta$, AC-αα$\delta\beta$, and AC-αα$\delta\gamma$, causing ~50% inhibition. Although in our preliminary analyses we observed AC-αα19 caused an approximate 50% inhibition of enzyme activity with the PP2A catalytic subunit from bovine cardiac muscle (*17*), we found no significant inhibition of oyster PP1 or PP2A (Table 2). Okadaic acid (100 μM) and calyculin A (10 nM) were highly effective in our assay and caused >99% inhibition of PP1 or PP2A activity (data not shown). Although no compound at 100 μM produced >60% inhibition of PP1 or PP2A (Table 2), a preference for compounds with aromatic substituents on R_3 and R_4 emerged for these PSTPases.

Table 3: Percent Inhibition of DSPase Activity with 100 μM Combinatorial Compound[a]

	Cdc25												MAPKP			
	Cdc25 A				Cdc25 B				Cdc25 C				CL100			
	exp. 1		exp. 2		exp. 1		exp. 2		exp. 1		exp. 2		exp. 1		exp. 2	
compound	mean	SEM	mean	SEM	mean	SEM	mean	SEM	mean	SEM	mean	SEM	mean	SEM	mean	SEM
AC-α119	35	3	30	1	0	0	0	0	6	3	0	0	10	3	5	6
AC-α169	86	2	86	2	53	1	60	1	11	1	28	1	16	4	21	5
AC-α1δ9	90	1	88	3	55	1	60	2	44	2	35	5	19	3	0	0
AC-αα19	0	0	3	2	9	2	8	1	33	2	21	2	0	0	18	6
AC-αα69	95	4	92	3	82	1	84	2	64	3	56	1	26	4	27	6
AC-ααδ9	97	2	97	1	84	1	87	5	56	3	60	2	0	0	12	10
AC-α11β	48	3	52	5	42	10	0	0	18	1	2	1	0	0	0	0
AC-α16β	70	2	58	4	44	4	18	3	17	2	14	2	0	0	0	0
AC-α1δβ	77	2	62	2	35	1	38	1	21	8	28	2	0	0	0	0
AC-αα1β	0	0	0	0	9	1	11	6	46	2	31	1	0	0	0	0
AC-αα6β	20	4	15	2	24	1	24	2	27	4	40	4	0	0	4	6
AC-ααδβ	48	1	29	1	30	2	32	3	57	5	51	2	0	0	0	0
AC-α11γ	85	4	77	1	53	1	57	1	54	1	52	2	0	0	0	0
AC-α16γ	78	5	64	1	34	1	34	3	30	2	33	1	0	0	0	0
AC-α1δγ	76	3	55	1	34	1	34	3	37	4	36	1	0	0	0	0
AC-αα1γ	31	3	27	4	7	5	20	3	48	2	51	2	0	0	4	6
AC-αα6γ	48	2	43	2	46	3	29	2	52	6	51	1	25	5	21	1
AC-ααδγ	73	2	43	3	57	3	31	6	66	3	56	3	0	0	0	0

[a] Each value is the percent inhibition from untreated control and the mean from an experiment done in triplicate.

Table 4: Percent Inhibition of PTPase Activity with Combinatorial Compound[a]

	3 μM		100 μM	
compound	mean	SEM	mean	SEM
AC-α119	0	0	32	7
AC-α169	15	6	77	7
AC-α1δ9	48	3	85	9
AC-αα19	3	7	38	10
AC-αα69	37	9	91	13
AC-ααδ9	40	2	92	3
AC-α11β	43	12	91	5
AC-α16β	50	7	61	14
AC-α1δβ	5	7	59	7
AC-αα1β	41	26	50	8
AC-αα6β	35	24	63	13
AC-ααδβ	3	10	1	16
AC-α11γ	0	0	45	3
AC-α16γ	38	3	74	8
AC-α1δγ	5	7	80	9
AC-αα1γ	41	26	52	7
AC-αα6γ	42	7	48	13
AC-ααδγ	42	7	79	12

[a] Each value is the percent inhibition from untreated control and the mean from at least three independent determinations.

Several library members also appeared to inhibit DSPases significantly at 100 μM (Table 3). Thus, AC-ααδ9 and AC-αα69 caused >90% inhibition of Cdc25A, AC-α169, AC-α1δ9, and AC-α11γ caused >80% inhibition of Cdc25A, while other compounds, such as AC-αα1β and AC-αα19, had no effect (Table 3). Minor structural modifications of the platform produced marked changes in inhibitory ability consistent with the concept of a restrictive catalytic site in Cdc25 as compared to the PTPase PTP1B. It was noteworthy, however, that the modification pattern for Cdc25 (Table 3) was distinct from that for PTP1B (Table 4).

In general, modification of the R_2 position produced minor changes with no obvious overall preference for phenyl versus methyl among the congeners for Cdc25 phosphatases. The best inhibitors of this series for Cdc25 phosphatases were found when both R_3 and R_4 contained hydrophobic moieties, such as aromatic or extended alkyl species. AC-αα69 and AC-αα6γ produced a modest (<30%) inhibition of CL100 activity at 100 μM, but all of the other members of the refined combinatorial library had little or no effect on this MAPK DSPase. Thus several compounds, such as AC-ααδ9, appeared to have some selectivity for the PTP1B PTPase and Cdc25 DSPases compared to either the MPKP DSPase CL100 or PSTPases.

Concentration Dependent Inhibition with Solid-Phase-Derived and SC Compounds. Analyses of combinatorial library elements required resynthesis of the predicted discrete compound with promising biochemical effects to ensure the inhibitory activity was not associated with a side reactant or contaminants (*23*). To investigate more extensively the inhibitory potential of the most active compounds against Cdc25, we next synthesized AC-ααδ9 and AC-αα69 by solution chemistry methods. As illustrated in Figure 2A−D, both solid-phase-derived AC-ααδ9 and solution phase derived SC-ααδ9 demonstrated a marked concentration-dependent inhibition of recombinant human Cdc25A and B activity. We observed a half-maximal inhibitory concentration (IC_{50}) of 75 μM for Cdc25A and -B when treated with AC-ααδ9, while SC-ααδ9 showed an IC_{50} of approximately 15 μM for Cdc25A and -B (Figure 2A and C). Thus, the SC compounds displayed a 5-fold greater inhibitory activity compared to the solid phase derived compounds, which could reflect the increased purity, the inclusion of *R* stereoisomers in the racemic SC compounds, or both. Similarly, both AC-αα69 and SC-αα69 samples caused a concentration-dependent inhibition of Cdc25A and -B with the racemic SC compound being approximately 5−6-fold more potent (Figure 2B and D). The widely used PTPase inhibitor vanadate had an IC_{50} of 1 μM for Cdc25A and -B in this assay. To ensure that SC-ααδ9 and SC-αα69 did not also gain significant activity against PSTPases, we tested these compounds against oyster (data not shown) and rabbit skeletal muscle (Figure 3) PP1 and PP2A catalytic subunit and observed no inhibition at 100 μM. We have seen no inhibition of calf intestine alkaline phosphatase activity with 100 μM of any of the combinatorial library members or with

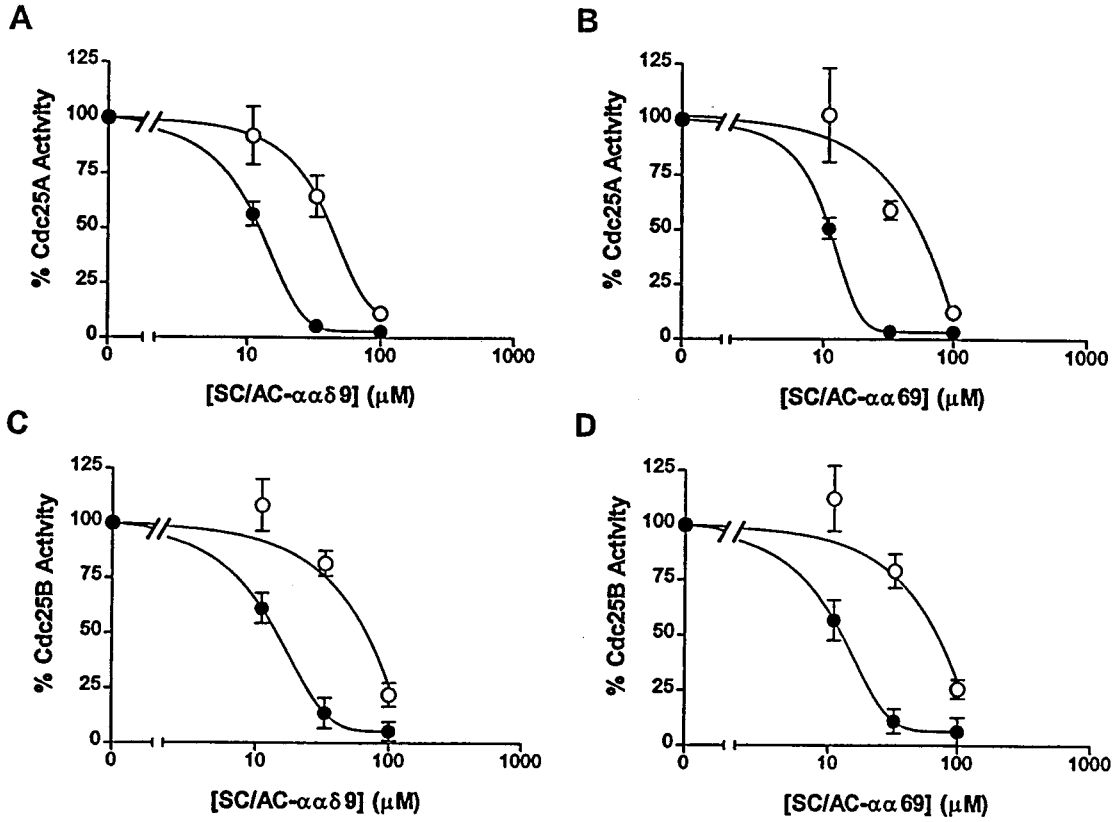

FIGURE 2: Concentration-dependent inhibition of Cdc25A and -B phosphatase by AC-ααδ9, SC-ααδ9, AC-αα69, and SC-αα69. Compounds AC-ααδ9 and AC-αα69 are indicated by open symbols and compounds SC-ααδ9 and SC-αα69 by closed symbols. (A) Inhibition of recombinant human Cdc25A phosphatase activity by SC-ααδ9 and AC-ααδ9. (B) Inhibition of recombinant human Cdc25A phosphatase activity by SC-αα69 and AC-αα69. (C) Inhibition of recombinant human Cdc25B phosphatase activity by SC-ααδ9 and AC-ααδ9. (D) Inhibition of recombinant human Cdc25B phosphatase activity by SC-αα69 and AC-αα69; $N = 3$; bar = SEM. Enzymatic activities were determined as outlined in Material and Methods and fit by the curve fitting program in Prism 2.01.

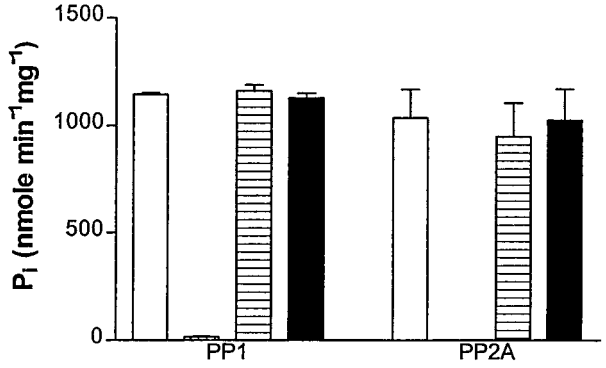

FIGURE 3: Inhibition of PP1 and PP2A by 100 μM SC-ααδ9 and SC-αα69. Controls are shown with open bars, cross-hatched bars represent 10 nM calyculin A treatment, and compounds SC-αα69 and SC-ααδ9 are indicated by horizontal and filled striped bars, respectively; $N = 3$; bar = SEM. Enzymatic activities were determined as outlined in the Material and Methods with rabbit skeletal muscle catalytic subunits.

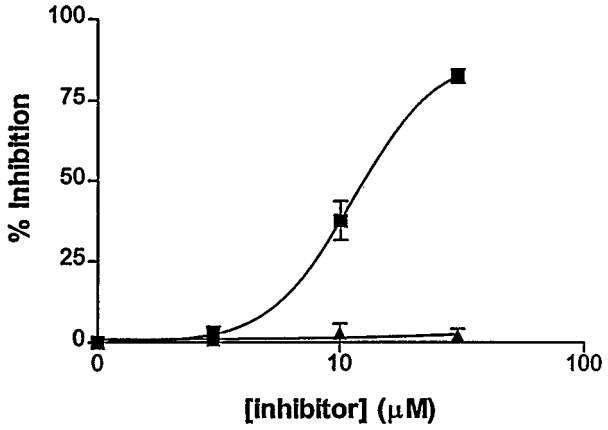

FIGURE 4: Effect of okadaic acid and SC-ααδ9 on Cdc25B phosphatase activity. Various concentrations of okadaic acid (▲) and SC-ααδ9 (■) were incubated with recombinant human Cdc25B as described in Material and Methods. The resulting data were fitted to the curve by Prism 2.01; $N = 3$; bar = SEM.

SC-ααδ9 or SC-αα69 (data not shown). Additionally, LeClerc and Meijer (personal communication) also found no inhibition of Cdc2 kinase activity as measure by their previously assay (*24*) with up to 100 μM SC-ααδ9. Furthermore, okadaic acid, a parent compound on which the pharmacophore platform was based, did not inhibit Cdc25B (Figure 4), demonstrating that the activity was not inherent in the parent compounds. To ensure that the inhibition was not dependent on the FDP substrate, we have also used pNPP as a substrate for Cdc25A and found marked inhibition with SC-ααδ9, although pNPP was a much poorer substrate than FDP (data not shown). These results confirm and extend studies of Gottlin et al. (*22*) indicating the aromatic substrate 3-*O*-methylfluorescein binds with higher affinity and reacts faster with Cdc25B than pNPP. In separate studies, LeClerc and Meijer (personal communication) have observed an IC_{50} of 4 μM with SC-ααδ9 and human recombinant Cdc25A using pNPP and their previously described method (*24*). Thus, the results with the solution phase compounds validated the initial observations with the combinatorial library.

Inhibition Kinetics of Compounds. We next determined the kinetic characteristics of DSPase and PTPase inhibition

Table 5: K_m and K_i of SC-ααδ9 and SC-αα69 for DSPases and PTPases

	K_m (μM)		K_i for SC-ααδ9 (μM)		K_i for SC-αα69 (μM)	
compound[a]	average	SEM	average	SEM	average	SEM
Cdc25A	45	3	9	2	8	3
Cdc25B	12	3	6	2	7	3
Cdc25C	22	1	11	3	11	2
CL100	192	72	229	115	ND[b]	ND
PTP1B	21	9	1.2	0.2	0.85	0.06

[a] $n = 3-10$ independent experiments. [b] ND, not determined.

with SC-ααδ9 and SC-αα69. We found the K_m with FDP for Cdc25A, Cdc25B, Cdc25C, CL100, and PTP1B were 45 ± 3 (SEM, $N =$ at least 4), 12 ± 3, 22 ± 1, 192 ± 72 and 21 ± 9 μM, respectively (Table 5). Therefore, FDP was a much better substrate for Cdc25 and PTP1B phosphatases than for the MAPK phosphatase CL100. Kinetic studies using SC-ααδ9 and SC-αα69 with Cdc25B were most consistent with a competitive inhibition model (Figure 5) while for PTP1B noncompetitive inhibition was the best model (Figure 6). We also concluded SC-ααδ9 competitively inhibits Cdc25A, Cdc25C and CL100 (data not shown) and SC-αα69 competitively inhibits Cdc25A and Cdc25C (data not shown). SC-αα69 had a K_i of 7 ± 3 μM for Cdc25B phosphatase and a K_i of 0.85 ± 0.06 μM for PTP1B (Table 5). The K_i for Cdc25A and Cdc25C were 8 ± 3 μM and 11 ± 2 μM, respectively (Table 5). The K_i for SC-ααδ9 for the MAPK phosphatase CL100 was 229 ± 115 μM. We have not yet determined the K_i for SC-αα69 and CL100.

On the basis of our initial studies with the library, we predicted that substitution of sterically enriched, hydrophobic moieties on this platform was critical for an efficient inhibitor of Cdc25 and PTP1B. To assess the relative importance of the bulky hydrophobic substitutents on the R_3 position, we synthesized two close congeners of SC-ααδ9 and SC-α1δ9, namely, SC-αα09 and SC-α109 (Figure 7A). SC-αα09 had markedly less inhibitory activity at 100 μM compared to SC-ααδ9, and SC-α109 also was less active than SC-α1δ9 (Figure 7B) indicating the importance of the bulky moiety in the R_3 position for Cdc25 phosphatase. SC-αα09 had the same strong inhibitory activity upon PTP1B as SC-ααδ9 demonstrating a bulky moiety at R_3 position was not critical for PTP1B inhibition (Figure 7C). Furthermore, both SC-αα09 and SC-ααδ9 produced similar inhibition of PTP1B of approximately 50% at 3 μM (data not shown).

Combinatorial chemistry provides a powerful new approach to diversify the structure of biologically active natural products (*23*). In this study we have developed a refined chemical scaffold for targeted combinatorial chemistry based on a predicted pharmacophore obtained from the structure activity relationship of several natural product inhibitors of PSTPases. Although the side chain composition and the size of the initial library are rather limited at this time, the

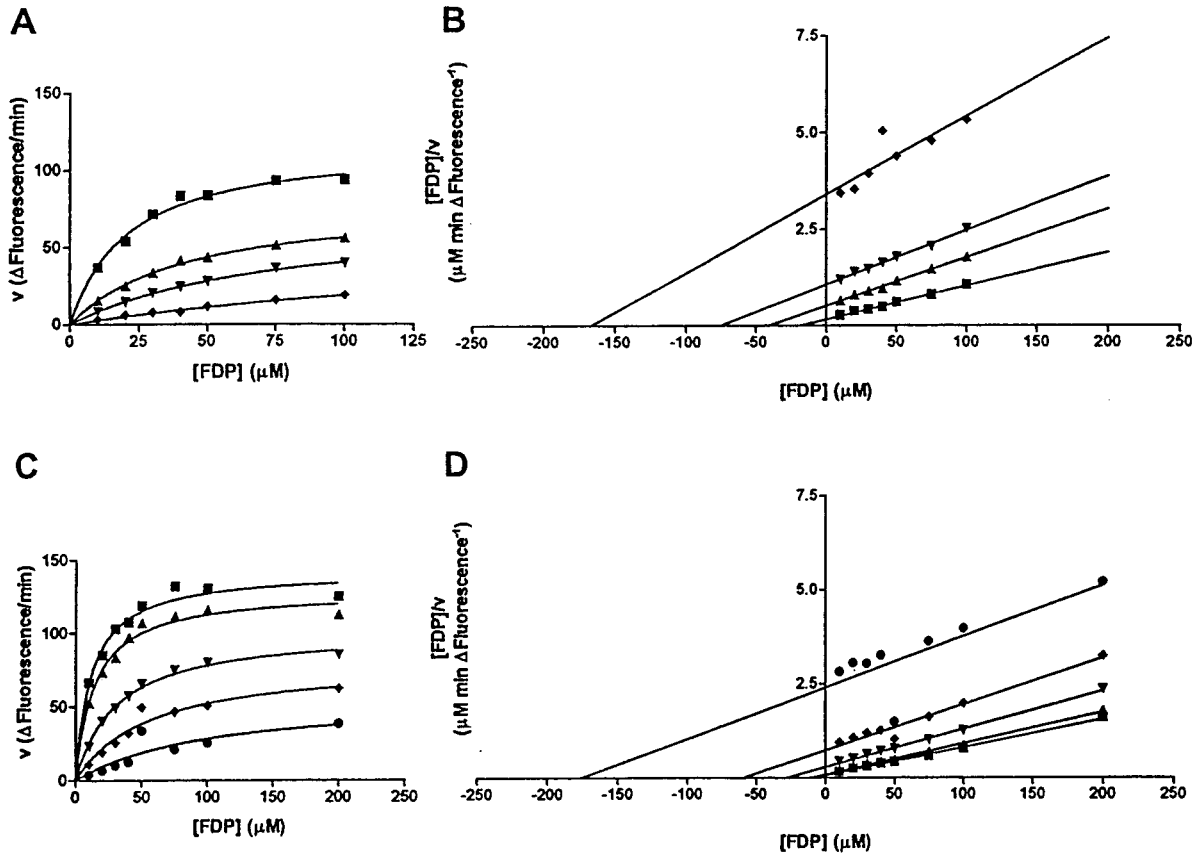

FIGURE 5: Kinetic analyses of Cdc25B inhibition by SC-ααδ9 and SC-αα69. (A, B) (■) 0 μM, (▲) 10 μM, (▼) 15 μM, and (◆) 30 μM inhibitor concentration. (C, D) (■) 0 μM, (▲) 3 μM, (▼) 10 μM, (◆) 15 μM, and (●) 30 μM inhibitor concentration. (A) Michaelis−Menten plot of Cdc25B inhibition by SC-ααδ9. (B) Hanes−Woolf plot of Cdc25B inhibition by SC-ααδ9. (C) Michaelis−Menten plot of Cdc25B inhibition by SC-αα69. (D) Hanes−Woolf plot of Cdc25B inhibition by SC-αα69; $N = 5$. Enzyme activities were determined as outlined in Materials and Methods, and the data were fit to the nonlinear Michaelis−Menten equation while all the data points were also fit simultaneously to the Hanes−Woolf equation for competitive inhibition for the Hanes−Woolf plot by the curve fitting program Prism 2.01. The values reported under Results for K_m and K_i were calculated from a nonlinear fit of the data to the Michaelis−Menten equation for competitive inhibition using the same program.

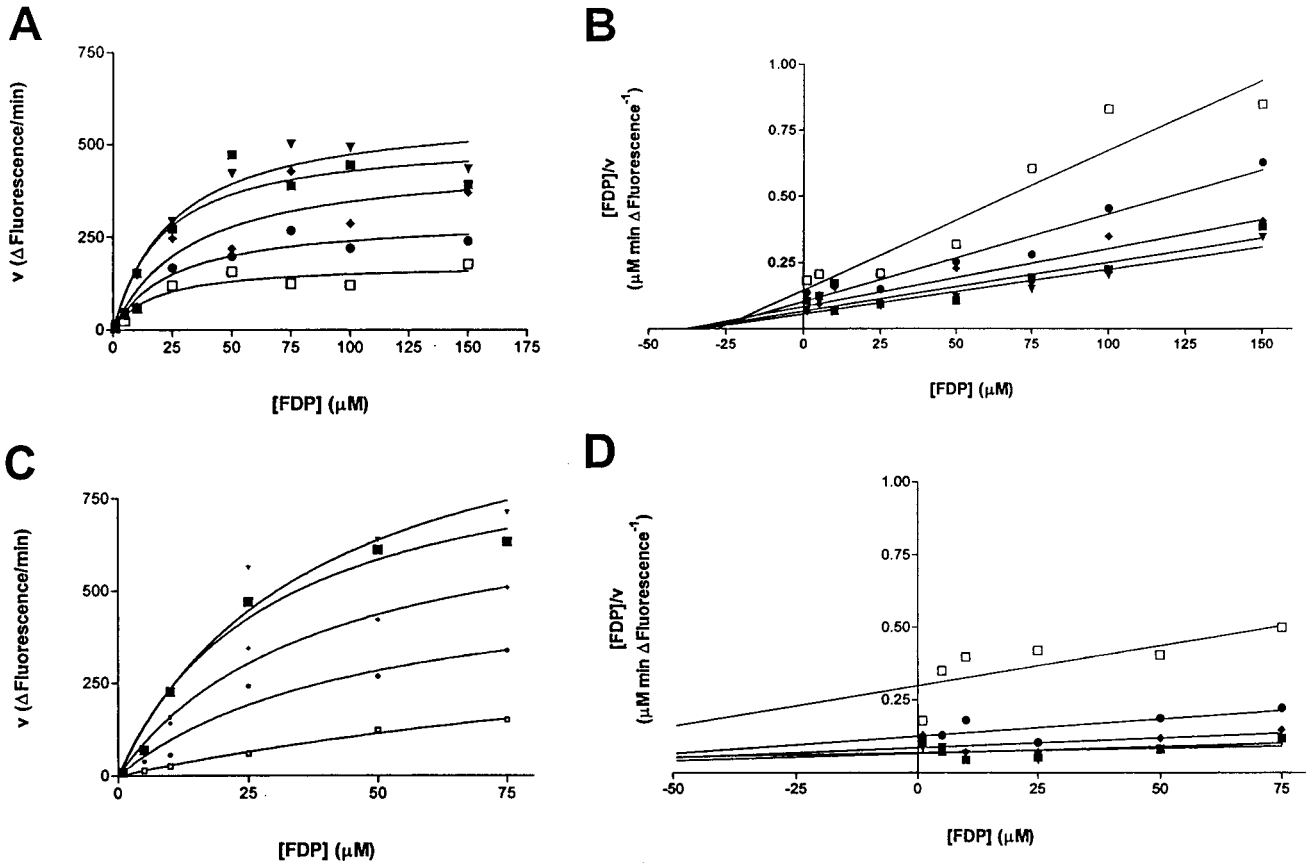

FIGURE 6: Kinetic analyses of PTP1B inhibition by SC-ααδ9 and SC-αα69. (A, B) (■) 0 μM, (▼) 0.1 mM, (◆) 0.3 μM, (●) 1 μM, and (□) 3 μM inhibitor concentration. (A) Michaelis−Menten plot of PTP1B inhibition by SC-ααδ9. (B) Hanes−Woolf plot of PTP1B inhibition by SC-ααδ9. (C) Michaelis−Menten plot of PTP1B inhibition by SC-αα69. (D) Hanes−Woolf plot of PTP1B inhibition by SC-αα69, $N = 4$. Enzyme activities were determined as outlined in Materials and Methods, and the data were fit to the nonlinear Michaelis−Menten equation while all the data points were also fit simultaneously to the Hanes−Woolf equation for competitive inhibition for the Hanes−Woolf plot by the curve fitting program Prism 2.01. The values reported under Results for K_m and K_i were calculated from a nonlinear fit of the data to the Michaelis−Menten equation for noncompetitive inhibition using the same program.

pharmacophore was readily functionalized and proved to be a most promising platform for future compound syntheses. It is noteworthy that none of the compounds in the library had highly efficacious inhibitory activity against PSTPases despite the use of a pharmacophore that owed its original design to natural product PSTPase inhibitors.

A detailed analysis of the structure−activity profile is limited by the relatively small library size; however, certain observations can be made concerning the inhibition of PSTPase, Cdc25 phosphatase and the PTPase PTP1B. Clearly the ability of some of the library compounds, such as AC-αα$\delta\beta$, to modestly inhibit both PP2A and Cdc25 phosphatases while having little effect on PTP1B indicates some overlapping inhibitor specificity between the PSTPases and Cdc25 enzyme. Nonetheless, distinct specificity emerged between PP2A phosphatase and the Cdc25 and PTP1B phosphatases, which might be expected considering the differences in the catalytic mechanisms in the broad PSTPase and PTPase families (*1*). The nonyl moiety has greater steric bulk and is more hydrophobic (log $P > 4$) compared to either the phenethyl (log $P = 3.15$) or styryl (log $P = 2.95$) moieties. Substitution of the nonyl moiety at the R_4 site of a compound containing a phenyl at R_2 and a benzyl at R_3 (Figure 1) caused a significant increase in Cdc25 phosphatase inhibition and a complete loss of PSTPase inhibition as compared to the substitution of the phenethyl or styryl moiety at R_4. This may reflect a hydrophobic region on Cdc25 near the active site. Interestingly, Sodeoka et al. (*11*) found the hydrophobic side chain of RK-682 was important for the inhibitory activity against Cdc25 but not VHR. In contrast to Cdc25 phosphatases, the PSTPases were much less tolerant of bulky, hydrophobic substitutions at R_4 and none of the R_4 nonyl compounds were effective inhibitor of PP1 or PP2A while AC-α169 and AC-α1δ9 were respectable inhibitors of Cdc25A and -B and PTP1B phosphatase (Tables 3 and 4). In contrast to the inhibitory profile with Cdc25 phosphatases, AC-ααδ9 and AC-αα$\delta\gamma$ reproducibly inhibited PTP1B equally well.

The identification of inhibitors that clearly prefer PTPases over PSTPases most likely reflects the lack of sequence similarity between these enzyme classes and the distinct fundamental catalytic mechanisms that exist between PSTPases and the enzyme superfamily of PTPases, which includes the DSPases (*1, 22, 25*). The crystal structure of the catalytic sites of prototype PSTPase, PTPases, and DSPases also suggests that they would accommodate different substrates and inhibitors consistent with previous biochemical studies (*1, 25, 26*). Consequently, the identification of inhibitors for the Cdc25 class of DSPase and the PTPase PTP1B is consistent with our current understanding of these phosphatases. Interestingly, these inhibitors were not very effective against the MAPK phosphatase class, which probably reflects the lack of common intervening amino acids in the critical HCXXXXXR active. Because

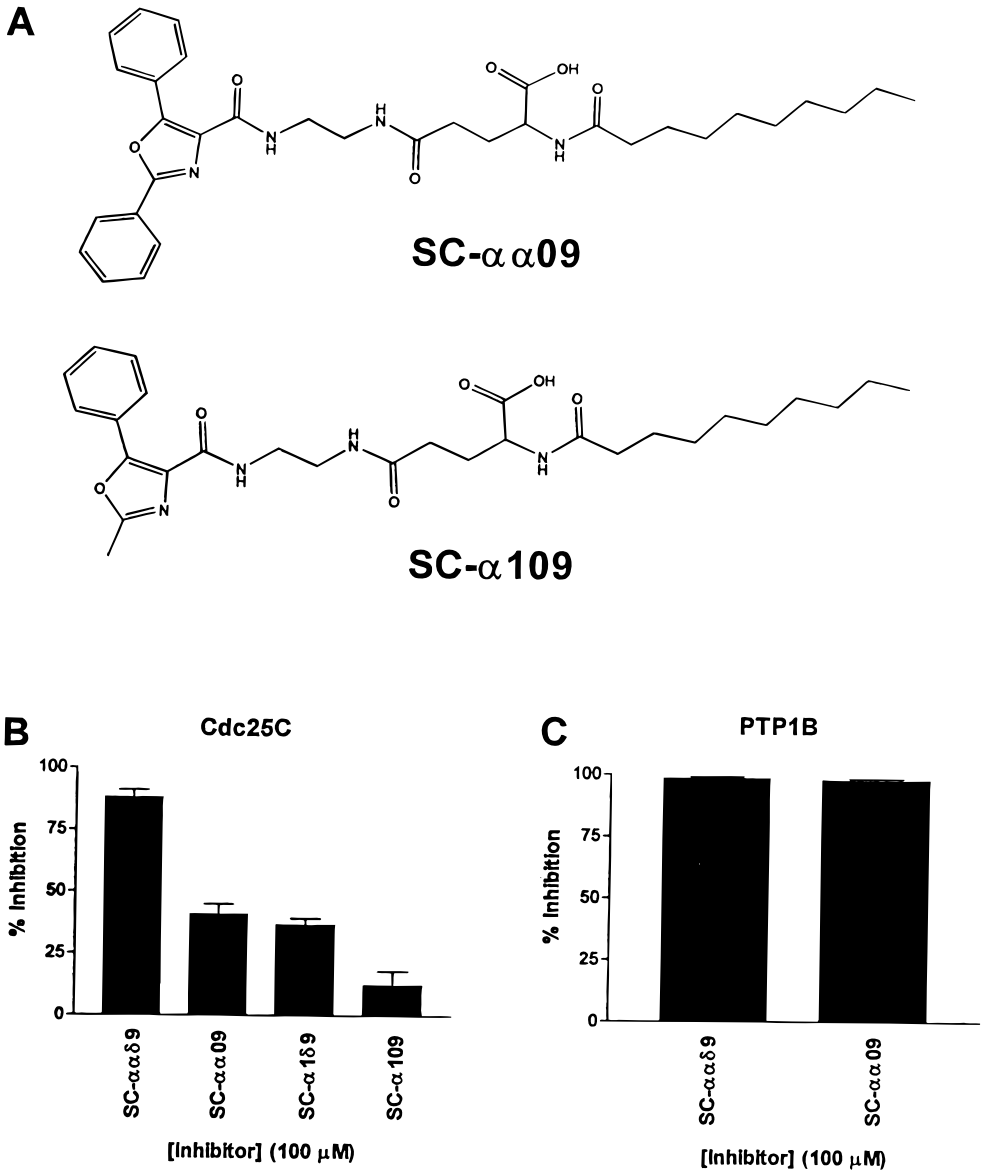

FIGURE 7: Chemical structure and inhibition of SC-αα09 and SC-α109. (A) Chemical structures of SC-αα09 and SC-α109. (B) Inhibition of Cdc25C phosphatase activity as described by the procedures in Materials and Methods. All values are expressed as a percent of vehicle control and the compound concentration was 100 μM; $N = 3$; bars = SEM. (C) Inhibition of PTP1B phosphatase activity as described by the procedures in the Materials and Methods. All values are expressed as a percent of vehicle control, and the compound concentration was 100 μM; $N = 3$; bars = SEM.

the catalytic regions of the Cdc25 enzymes, namely HCEF-SSER, are identical, the similar K_i values for Cdc25A, -B, or -C with SC-ααδ9 or SC-αα69 are not surprising.

In summary, we have identified a new class of small-molecule, competitive, inhibitors of human Cdc25 DSPases and noncompetitive inhibitors of PTP1B PTPase that are readily synthesized. Moreover, there is some evidence that PP2A and Cdc25 phosphatases have overlapping yet distinct inhibitor specificity. These compounds are small and have chemical structures unlike known PTP1B or Cdc25 inhibitors (*10*, *11*, *12*, *27*). We previously demonstrated (*17*) that AC-ααδ9 caused a concentration-dependent inhibition of human breast cancer MDA-MB-21 cell proliferation and a G_1 cell cycle block consistent with intracellular entry. We are currently attempting to determine if these cellular effects are mediated by phosphatase inhibition. The pharmacophore used in our present studies should provide an excellent platform for future analog development. Our results illustrate the potential usefulness of this combinatorial-based approach in generating lead structures for selective inhibitors for phosphatases.

ACKNOWLEDGMENT

We are grateful for the constructive comments of Drs. Guillermo Romero and Andreas Vogt (University of Pittsburgh). We also thank Drs. LeClerc and Meijer (CNRS, Roscoff, France) for assaying our compounds, Dr. Stephen M. Keyse (University of Dundee, U.K.), Dr. Jehangir Mistry (Diagnostic Systems Labs, Webster, TX) for TLC advice, Dr. David Beach (Cold Spring Harbor Laboratories, NY), and Robert T. Abraham (Mayo Clinic) for reagents used in these studies, and Mark Stroud (Northwest Hospital) for his technical assistance with the PP1 and PP2A assay.

REFERENCES

1. Denu, J. M., Stuckey, J. A., Saper, M. A., and Dixon, J. E. (1996) *Cell 87*, 361−364.

2. Honkanen, R. E., Zwiller, J., Moore, R. E., Daily, S. L., Khatra, B. S., Dukelow, M., and Boynton, A. L. (1990) *J. Biol. Chem. 265*, 19401−19404.
3. Takai, A., Sasaki, K., Nagai, H., Mieskes, G., Isobe, M., Isono, K., and Yasumoto, T. (1995) *Biochem. J. 306*, 657−665.
4. Yoshizawa, S., Matsushima, R., Watanabe, M. F., Harada, K., Ichihara, A., Carmichael, W. W., and Fujiki, H. (1990) *J. Cancer Res. Clin. Oncol. 116*, 609−614.
5. MacKintosh, C., and Klumpp, S. (1990) *FEBS Lett. 277*, 137−140.
6. Keyse, S. M., and Emslie, E. A. (1992) *Nature 359*, 644−647.
7. Schmidt, A., Rutledge, S. J., Endo, N., Opas, E. E., Tanaka, H., Wesolowski, G., Leu, C. T., Huang, Z., Ramachandaran, C., Rodan, S. B., and Rodan, G. A. (1996) *Proc. Nat. Acad. Sci. U.S.A. 93*, 3068−3073.
8. Groom, L. A., Sneddon, A. A., Alessi, D. R., Dowd, S., and Keyse, S. M. (1996) *EMBO J. 15*, 3621−3632.
9. Horiguchi, T., Nishi, K., Hakoda, S., Tanida, S., Nagata, A., and Okayama, H. (1994) *Biochem. Pharmacol. 48*, 2139−2141.
10. Gunasekera, S. P., McCarthy, P. J., and Kelly-Borges, M. (1996) *J. Am. Chem. Soc. 118*, 8759−8760.
11. Sodeoka, M., Sampe, R., Kagamizono, T., and Osada, H. (1996) *Tetrahedron Lett. 37*, 8775−8778.
12. Akamatsu, M., Roller, P. P., Chen, L., Zhang, Z. Y., Ye, B. and Burke, T. R., Jr. (1997) *Bioorg. Med. Chem. 5*, 157−163.
13. Chen, L., Montserat, J., Lawrence, D. S., and Zhang, Z. Y. (1996) *Biochemistry 35*, 9349−9354.
14. Eckstein, J. W., Beer-Romero, P., and Berdo, I. (1996) *Protein Sci. 5*, 5−12.
15. Quinn, R. J., Taylor, C., Suganuma, M., and Fujiki, H. (1993) *Bioorg. Med. Chem. Lett. 3*, 1029−1034.
16. Bell, J. R., Ollivier, Emmanuelle, O., and Guerucci, M.-A. (1992) *Biol. Cell 75*, 139−142.
17. Wipf, P., Cunningham, A., Rice, R. L., and Lazo, J. S. (1997) *Bioorg. Med. Chem. 5*, 165−178.
18. Coste, J., Frerot, E., and Jouin, P. (1994) *J. Org. Chem. 59*, 2437−2446.
19. Shioiri, T., Ninomiya, K., and Yamada, S. (1972) *J. Am. Chem. Soc. 94*, 6203−6205.
20. Honkanen, R. E., Codispoti, B., Tse, K., and Boynton, A. L. (1994) *Toxicon 32*, 339−350.
21. Honkanen, R. E., Dukelow, M., Zwiller, J., Moore, R. E., Khatra, B. S., and Boynton, A. L. (1991) *Mol. Pharmacol. 40*, 577−583.
22. Gottlin, E. B., Xu, X., Epstein, D. M., Burke, S. P., Eckstein, J. W., Ballou, D. P., and Dixon, J. E. (1996) *J. Biol. Chem. 271*, 27445−27449.
23. Ellman, J., Stoddard, B., and Wells, J. (1997) *Proc. Natl. Acad. Sci. U.S.A. 94*, 2779−2782.
24. Baratte, B., Meijer, L., Galaktionov, K., and Beach, D. (1992) *Anticancer Res. 12*, 873−880.
25. Yuvaniyama, J., Denu, J. M., Dixon, J. E., and Saper, M. A. (1996) *Science 272*, 1328−133.
26. Draetta, G., and Eckstein, J. (1997) *Biochem. Biophys. Acta 1332*, M53−M63.
27. Watanabe, T., Takeuchi, T., Otsuka, M., Tanaka, S. I., and Umezawa, K. (1995) *J. Antibiotics 48*, 1460−1466.

BI971338H